Geophysical Research Letters

RESEARCH LETTER
10.1029/2024GL110457

Why Is Decadal Climate Variability Predominantly Observed in the Niño4 Region?

Sieu-Cuong San[1], Yu-Heng Tseng[1,2], Ruiqiang Ding[3], and Emanuele Di Lorenzo[4]

[1]Institute of Oceanography, National Taiwan University, Taipei, Taiwan, [2]Ocean Center, National Taiwan University, Taipei, Taiwan, [3]State Key Laboratory of Earth Surface Processes and Resource Ecology, Beijing Normal University, Beijing, China, [4]Department of Earth, Environmental, and Planetary Sciences, Brown University, Providence, RI, USA

Key Points:

- Subsurface temperature anomalies initiate the phase reversal of TPDV while PMM plays a key role in equatorial SSTAs post-transition
- Vertical heat advection is crucial in reinforcing/weakening decadal variance in the Niño4/Niño3 region
- PMM-associated wind fields induce anomalous vertical advection after the TPDV phase transition

Supporting Information:

Supporting Information may be found in the online version of this article.

Correspondence to:

Y.-H. Tseng,
tsengyh@ntu.edu.tw

Citation:

San, S.-C., Tseng, Y.-H., Ding, R., & Di Lorenzo, E. (2024). Why is Decadal Climate Variability predominantly observed in the Niño4 region? *Geophysical Research Letters*, *51*, e2024GL110457. https://doi.org/10.1029/2024GL110457

Received 1 JUN 2024
Accepted 14 AUG 2024

Abstract This study investigates why observed decadal-scale climate variability is predominantly pronounced in the Niño4 region compared to other equatorial Pacific areas using both observation and model sensitivity experiments. The initial shift to the negative phase of Tropical Pacific Decadal Variability (TPDV) is primarily driven by the upward and eastward migration of isopycnal negative temperature anomalies along the equator. Subsequently, the wind fields associated with the negative phase of the Pacific Meridional Mode (PMM) induce anomalous vertical currents in the equatorial Pacific. This leads to anomalous upwelling and downwelling of mean temperature in the Niño4 and Niño3 regions, respectively, thereby strengthening and weakening the corresponding subsurface-produced sea surface temperature anomalies. Our findings clarify the roles of subsurface temperature anomalies in the phase reversal of TPDV and PMM in amplifying decadal variance, specifically in the equatorial central Pacific.

Plain Language Summary Observations have consistently highlighted prominent decadal climate variability in the Niño4 region, yet the underlying cause of this distinct pattern remains largely elusive. In this study, we use composite analysis during the phase transition of Tropical Pacific Decadal Variability (TPDV) and modeling experiments to elucidate the mechanisms governing the observed decadal climate variability in the Niño4 region compared to other equatorial areas. Our findings reveal that the eastward and upward propagation of negative subsurface temperature anomalies primarily drives the phase reversal of TPDV. Following this transition from positive to negative phase, the Pacific Meridional Mode (PMM) plays a crucial role. Specifically, PMM-associated wind forcing induces anomalous upwelling and downwelling in the Niño4 and Niño3 regions, respectively. This results in anomalous vertical advection of mean temperature, contributing to the strengthening and weakening of decadal variances in these regions.

1. Introduction

Tropical Pacific Decadal Variability (TPDV) is a natural climate phenomenon occurring on timescales greater than 7 years in the Pacific (Capotondi et al., 2023; Z. Liu & Di Lorenzo, 2018; Y. Zhao & Di Lorenzo, 2020). TPDV gains significant attention in climate research (Capotondi et al., 2023; Z. Liu, 2012; Power et al., 2021) due to its substantial impact on global climate patterns and extreme weather events (Liu et al., 2019; Okumura, DiNezio, & Deser, 2017; Wang et al., 2010, 2011, 2014; Zhang et al., 2016). Additionally, it may interact with one of the most influential interannual phenomena on Earth, the El Niño Southern Oscillation (ENSO) (Fedorov & Philander, 2000; McPhaden et al., 2011; Okumura, Sun, & Wu, 2017; Sun & Okumura, 2020; Zhao et al., 2016; Zhong et al., 2017). Unlike ENSO, which exhibits large interannual variance from the central to the eastern equatorial Pacific (Timmermann et al., 2018), the strongest variance of TPDV extends from the northeastern subtropic to the equatorial central Pacific, particularly in the Niño4 region (Figure S1a in Supporting Information S1) (Capotondi et al., 2022; Chunhan et al., 2021; Di Lorenzo et al., 2023; Liu et al., 2022). This spatial structure bears resemblance to the Central Pacific ENSO (Ashok et al., 2007; Capotondi et al., 2022; Sullivan et al., 2016) and the Pacific Meridional Mode (PMM) (Amaya, 2019; Chiang & Vimont, 2004; Stuecker, 2018), suggesting a significant contribution of PMM to TPDV dynamics (Di Lorenzo et al., 2015; Joh & Di Lorenzo, 2019; Zhao et al., 2023). However, why the decadal variance of TPDV is most prominent in the equatorial central Pacific remains unclear (Figures S1 and S2 in Supporting Information S1). Further investigation is needed to clarify the physical processes responsible for this observed decadal variability.

Several mechanisms have been proposed to explain the temporal and spatial characteristics of TPDV (Capotondi et al., 2023; Power et al., 2021). The substantial variance observed in the equatorial central Pacific could potentially stem from residual effects of interannual ENSO events (Vimont, 2005) or nonlinearities inherent in ENSO dynamics (Cibot et al., 2005; Kim & Kug, 2020; Rodgers et al., 2004). The preferred timescale of TPDV appears to be established through the adjustment of the subtropical-tropical cells (STCs) (Z. Liu, 1994; McCreary & Lu, 1994) associated with the propagation of oceanic Rossby waves (Capotondi & Alexander, 2001; Capotondi et al., 2003; Knutson & Manabe, 1998; Meehl & Hu, 2006), the mean advection of density-compensated temperature and salinity anomalies originating from the eastern subtropical Pacific (Gu & Philander, 1997; San & Tseng, 2024; Schneider, 2000; Tatebe et al., 2013; Zeller et al., 2021), and extratropical-tropical ocean-atmosphere coupling (Joh & Di Lorenzo, 2019). Regarding the phase transition of TPDV, proposed mechanisms include ENSO nonlinear dynamical heating (Liu et al., 2022), the combined influence of large decadal timescale heat content anomalies in the off-equatorial western tropical Pacific and the onset of ENSO events (Meehl et al., 2021), and potential influences from the Atlantic and Indian Oceans (Cai et al., 2019; Li et al., 2016; Luo et al., 2012; McGregor et al., 2014). Although these mechanisms offer valuable insights, the actual contributions of each remain unclear. Furthermore, a comprehensive framework explaining TPDV's origin, preferred timescale, and phase transition remains largely inconclusive.

A recent study has demonstrated that off-equatorial northwestern Pacific subsurface temperature anomalies and extratropical-tropical ocean-atmosphere coupling can well explain both the phase transition and preferred timescale of TPDV (San et al., 2024). Specifically, the TPDV positive phase induces anomalous circulation in the off-equatorial western and extratropical Pacific (Alexander et al., 2002; Z. Liu & Alexander, 2007; Meehl et al., 2021; Trenberth et al., 1998). The former generates an off-equatorial northwest center of negative subsurface temperature anomalies due to surface divergence (Meehl et al., 2021) while the latter potentially induces Kuroshio Extension (KE) state change due to westward propagating oceanic Rossby waves (Andres et al., 2009; Ceballos et al., 2009; Taguchi et al., 2007). The northwestern subsurface temperature anomalies then follow the North Equatorial Countercurrent (NECC) pathway toward the central basin (Zhang et al., 1999; R. Zhang & Rothstein, 2000), shoaling upward and eastward along the equator to reverse the sign of the sea surface temperature (SST) anomalies (SSTAs) at the Niño4 region around 3 years later (San et al., 2024). Furthermore, the KE state change subsequently projects on the forcing of the PMM (Gan et al., 2023; Qiu et al., 2007, 2014; Wills & Thompson, 2018), further strengthening the subsurface-produced equatorial SSTAs within 1 year before the peak phase (Di Lorenzo et al., 2015; Joh & Di Lorenzo, 2019). Approximately 5 years later, the tropical Pacific ocean-atmosphere system completes its phase reversal into the mature cold phase. While this framework provides valuable insights into preferred oscillation timescale and phase transition (San et al., 2024), critical questions remain. How does the PMM contribute to strengthening equatorial SSTAs within 0–12 months before the peak phase? Is this process linked directly to thermodynamical (Vimont et al., 2001, 2003; Xie & Philander, 1994) and/or dynamical (Anderson et al., 2013; Anderson & Perez, 2015; Clarke et al., 2007) mechanisms, similar to those on interannual timescales (Yu & Fang, 2018)? Moreover, given that subsurface temperature anomalies originating in the off-equatorial northwestern Pacific shoal upward and eastward along the equator (Figure S3a in Supporting Information S1), one would expect these anomalies to potentially induce large decadal variability in the Niño3 region as well. However, the question arises: why is the observed decadal variance most pronounced in the Niño4 region rather than the Niño3 region?

In this study, we employ both observational data and model experiments to distinguish the distinct roles of subsurface temperature anomalies and PMM in driving TPDV dynamics. While subsurface temperature anomalies are crucial for the phase reversal of TPDV, PMM amplifies the subsurface-induced SSTAs in the Niño4 region while suppressing decadal variance in the Niño3 region by altering anomalous vertical advection following the TPDV phase transition. This resolves the important puzzles related to decadal-scale climate variability. The subsequent sections of this paper are structured as follows: Section 2 and Section 3 provide details on the data and methodology, respectively. Section 4 presents our main findings and Section 5 offers a summary and discussion of the results.

2. Data

Monthly SST data on a global 1° × 1° longitude-latitude grid are from the Hadley Center Global Sea Ice and Sea Surface Temperature dataset version 1.1 (Rayner et al., 2003). Monthly subsurface 1° ocean temperature data from the latest EN.4.2.2 dataset of the Met Office Hadley Center is provided over 42 irregularly spaced depth

levels spanning from 1900 to the present (Good et al., 2013). For atmospheric variables, we used monthly sea level pressure (SLP) and 10 m winds from the National Centers for Environmental Prediction-National Center for Atmospheric Research Reanalysis 1, which covers the period from 1948 to the present and is distributed on a 2.5° × 2.5° longitude-latitude grid (Kalnay et al., 1996). Additionally, the Estimating the Circulation and Climate of the Ocean project, version 3 (GECCO3) is used for heat budget analysis (Köhl, 2020). This dataset has 1° horizontal resolutions and 40 vertical levels, spanning from 1948 to 2018. Before conducting analyses, all data are linearly detrended, and anomalies are defined as deviations from the climatology of the entire period covered by the respective dataset. To isolate decadal-scale variability, we apply an 8–20 year Lanczos bandpass filter (Duchon, 1979). Our analysis focuses on the period from 1948 to 2023.

3. Methods

3.1. Composite Analysis

Following Meehl et al. (2021), we use composite analysis to investigate the atmospheric and oceanic variability during the phase transition of TPDV. The TPDV phase transition is defined as the time when the TPDV index, calculated as the 8–20 years bandpass filtered SSTAs in the Niño4 region (Liu et al., 2022; San et al., 2024), crosses the zero line. We identify six cases of TPDV transitioning from positive to negative, and an equal number of cases transitioning from negative to positive (Figure S2a in Supporting Information S1).

3.2. Heat Budget Analysis

Following Lee et al. (2004) and X. Zhang and McPhaden (2010), we analyze the heat budget in the Niño4 and Niño3 regions with a fixed bottom depth of 90 m to quantify the role of oceanic processes (Hayashi & Jin, 2017) during the phase transition of TPDV (Note that the results do not change if the fixed bottom depth is greater or smaller than 90 m). The heat budget equation is expressed as:

$$\frac{\partial T}{\partial t} = Q_{adv} + \frac{Q_{net}}{\rho C_p H} + R = Q_{advB} + Q_{advW} + Q_{advE} + Q_{advN} + Q_{advS} + \frac{Q_{net}}{\rho C_p H} + R \quad (1)$$

where T denotes the box-averaged temperature, Q_{adv} represents the net oceanic advection of temperature into the defined equatorial box from the bottom (Q_{advB}), western (Q_{advW}), eastern (Q_{advE}), northern (Q_{advN}), and southern (Q_{advS}) boundaries. Q_{net} indicates the net downward heat flux at the ocean surface and R denotes the residual term. Here, H is taken as a constant of 90 m, ρ, and C_p are constants of 1,025 kg m^{-3} and 3,940 J kg^{-1} K^{-1}, respectively.

4. Results

4.1. Features Observed During the Decadal Transition of Tropical Pacific Climate

We present the composite temporal evolution of various oceanic and atmospheric fields relevant to TPDV transitioning from positive to negative phases (similar results are obtained for the negative to positive transition albeit with reversed signs). Before the transition (−6 months, Figure 1a), we observe comparable magnitudes of positive SSTAs in the equatorial and subtropical northeastern and southeastern Pacific. In addition, significant negative SSTAs become prominent only in these regions about 1 year before the peak cold phase of TPDV (Figure 1d–1f). This suggests that while the PMM is not the primary driver of the TPDV phase reversal, it does play a significant role in strengthening equatorial SSTAs (Figure S4b in Supporting Information S1), consistent with previous studies (Di Lorenzo et al., 2015; Ding et al., 2022; Joh & Di Lorenzo, 2019). Furthermore, an anti-cyclonic large-scale circulation anomaly in the North Pacific, featuring a weakened Aleutian Low-like structure, emerges only after the TPDV transition which may play a dominant role in forcing the PMM to drive TPDV toward the mature cold phase (Figures S5d-S5f in Supporting Information S1) (San et al., 2024).

The composite temporal evolution of temperature anomalies averaged between 22 and 24.5 σ_θ reveals significant negative subsurface temperature anomalies before the transition (Figure S6a in Supporting Information S1), which continue to intensify until the peak cold phase of TPDV (Figures S6c–S6f in Supporting Information S1). These subsurface anomalies can propagate toward the equatorial central basin via the NECC pathway (Figure 1h and Figure S6b in Supporting Information S1) (San et al., 2024), ultimately leading to a reversal in the sign of SSTAs in the Niño4 region (light violet box in Figure 1b). Additionally, as the isopycnals outcrop along the

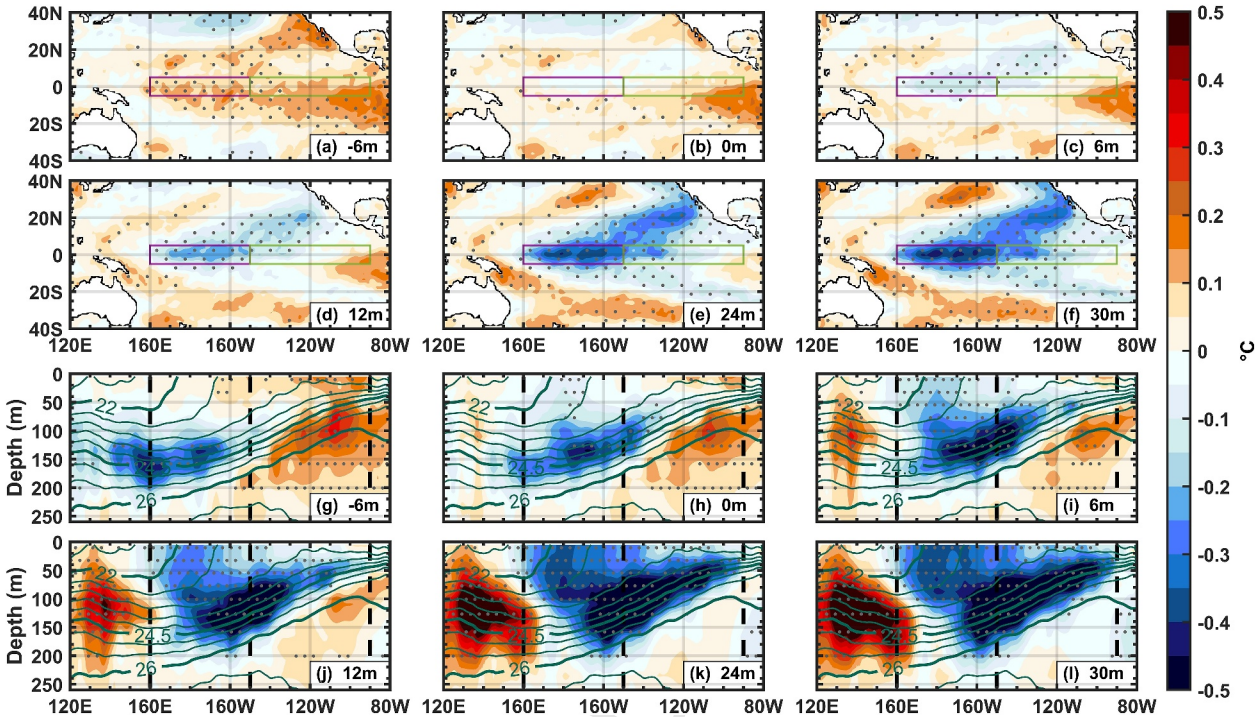

Figure 1. Composite evolution of 8–20 years bandpass filtered (a–f) SSTAs and (g–l) temperature anomalies averaged between 5°S and 5°N from the positive to negative phase transition. The months preceding the transition are indicated by negative values (e.g., −6 m represents 6 months prior to a transition) while months following the transition are indicated by positive values (e.g., 6 m indicates 6 months after a transition). Green contours in (g–l) indicate the long-term mean potential density averaged between 5°S and 5°N. The light violet and green rectangular boxes in (a–f) represent the Niño4 and Niño3 regions, respectively. Vertical dashed thick black lines in (g–l) mark the longitudes of 160°E, 150°W and 90°W. Stippling indicates regions where the anomalies are statistically significant at the 95% confidence level based on a Student's *t*-test.

equator (violet contours in Figure S3a in Supporting Information S1), subsurface temperature anomalies could also induce significant decadal variability in the Niño3 region (Figure S3c in Supporting Information S1). However, observations indicate that these anomalies intensify locally in the upper 200 m of the Niño4 region (Figures 1i–1l and S3b in Supporting Information S1) while large temperature anomalies are confined beneath the surface layer in the Niño3 region between 50 and 150 m depth (Figure S3c in Supporting Information S1). This vertical structure of temperature anomalies (Figure S3 in Supporting Information S1) is consistent with the spatial distribution of temperature variances shown in Figure S1 in Supporting Information S1, suggesting that understanding the physical mechanism during the phase transition is key to explaining the distribution of decadal variance in the equatorial Pacific. Figure 2 shows the distinct subsurface oceanic circulation features averaged within the longitudinal bands of the Niño4 (160°E-150°W) and Niño3 (150°W-90°W) regions. Following the transition, a notable upward motion of anomalous currents is observed in the Niño4 region (Figures 2d–2f and Figures S7d–S7f in Supporting Information S1), whereas the anomalous current pattern in the Niño3 region predominantly circulates downward in a clockwise manner centered at 60 m depth (Figures 2j–2l and Figures S7d–S7f in Supporting Information S1). These subsurface characteristics may relate to the contrasting wind fields in the Niño4 and Niño3 regions after the transition (Figures S5d–S5f in Supporting Information S1). Similar results are obtained using different reanalysis datasets, such as Ocean Reanalysis System 5 (ORAS5 (Zuo et al., 2019), Figure S8 in Supporting Information S1). Consequently, the anomalous currents can further amplify the subsurface-produced decadal signal in the Niño4 through anomalous upwelling of mean temperature (shading in Figures 2d–2f), while they tend to dampen the decadal signal by isolating it away from the surface in the Niño3 region (shading in Figures 2j–2l). These characteristics suggest that subsurface oceanic dynamics play a pivotal role in explaining why the decadal signals are more prominent in the Niño4 compared to the Niño3 region (cf., Figures S2a–S2f in Supporting Information S1). More details will be provided in the subsequent section.

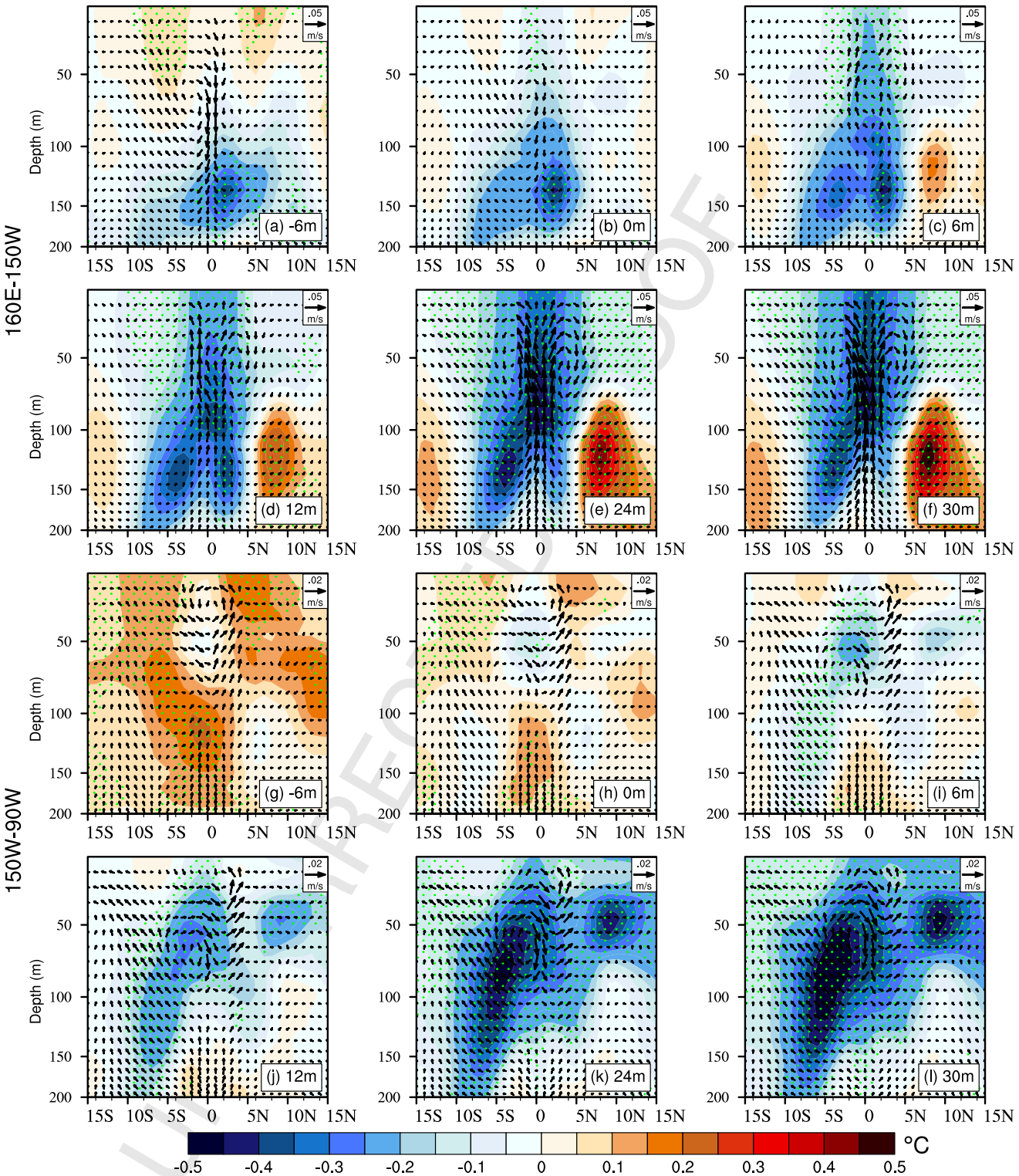

Figure 2. Same as Figure 1 but for temperature anomalies (shading), meridional and vertical (5×10^4) currents averaged between (a–f) 160°E-150°W and (g–l) 150°W-90°W. Stippling indicates regions where the temperature anomalies are statistically significant at the 95% confidence level based on a Student's *t*-test.

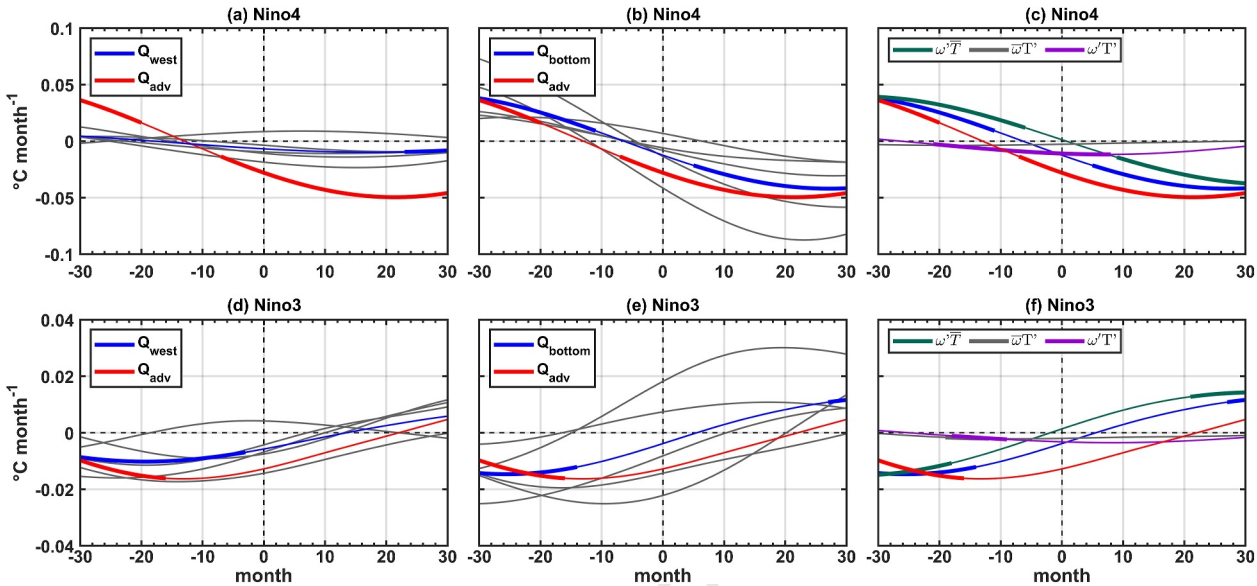

Figure 3. Composite evolution of heat advection into the (a)–(c) Niño4 and (d)–(f) Niño3 regions. In (a), the red and blue lines indicate the total heat advection and contribution through the western boundary, respectively. The gray lines depict the individual evolution (five cases) of heat advection through the western boundary. (b) Same as (a) but for the contribution through the bottom. (c) Decomposition of vertical heat transport (blue) into the anomalous upwelling of mean temperature (green), mean upwelling of anomalous temperature (gray), and anomalous upwelling of temperature anomalies (violet). The red line corresponds to (a). (d)–(f) Same as (a)–(c) but for the Niño3 region. In all panels, thick lines denote significance at the 95% level based on a Student's *t*-test.

4.2. The Physical Causes of Prominent Decadal Climate Variability in the Niño4 Region

The physical mechanisms driving notable decadal climate variability in the tropical Pacific are further explored through a heat budget analysis for the Niño4 and Niño3 regions, respectively. The heat budget closure shows a very small residual, with the sum of the first six terms on the right-hand side of Equation 1 closely matching the temperature tendency for both regions (corr. >0.99, Figure S9 in Supporting Information S1). Subsequently, we decompose the total heat advection term into contributions from individual boundary interfaces of the defined equatorial region (the first five terms in Equation 1). Heat advection into the Niño4 region is primarily driven by advection through the bottom at both interannual and decadal timescale (Figure S10 in Supporting Information S1). In contrast, heat advection into the Niño3 region comes from both the bottom and the western boundary (Figure S11 in Supporting Information S1), consistent with previous studies (Boucharel et al., 2015; Huang et al., 2012; Vialard et al., 2001). We further identify the dominant components of vertical and zonal temperature advection. In the Niño4 region, vertical heat advection is mainly driven by anomalous upwelling of mean temperature (Ekman feedback) while the contribution to the western boundary comes primarily from anomalous zonal advection of mean temperature and nonlinear zonal advection (Figures S12a and S13a in Supporting Information S1). In the Niño3 region, vertical heat advection is dominated by anomalous upwelling of mean temperature at the decadal timescale, while the contribution to the western boundary is primarily dominated by anomalous zonal advection of mean temperature (Figures S12b and S13b in Supporting Information S1).

The above analysis can further help us to quantify the contribution of key oceanic dynamics to tropical Pacific climate transitions. Figure 3 shows the composite temporal evolution of heat advection during the transition of TPDV from positive to negative phases. Following the transition, we observe that the transport through the bottom varies in phase and contributes significantly to the total heat advection in the Niño4 region (Figure 3b), consistent with the study of Zhang et al. (2022). Here, the predominant component of vertical heat transport is the anomalous upwelling of mean temperature (green line in Figure 3c), which reinforces the decadal signal (the light violet box in Figures 1e and 1f; the region between the first two vertical dashed lines in Figures 1k and 1l). In contrast, advection from the western boundary and vertical transport in the Niño3 region weaken the total heat advection and can even cause it to become positive around 2 years after the transition (Figures 3d and 3e), wherein the anomalous downwelling of mean temperature (green line in Figure 3f) and the anomalous zonal advection of mean temperature are the two most important components (not shown). Consequently, this dampens the decadal signal in the Niño3

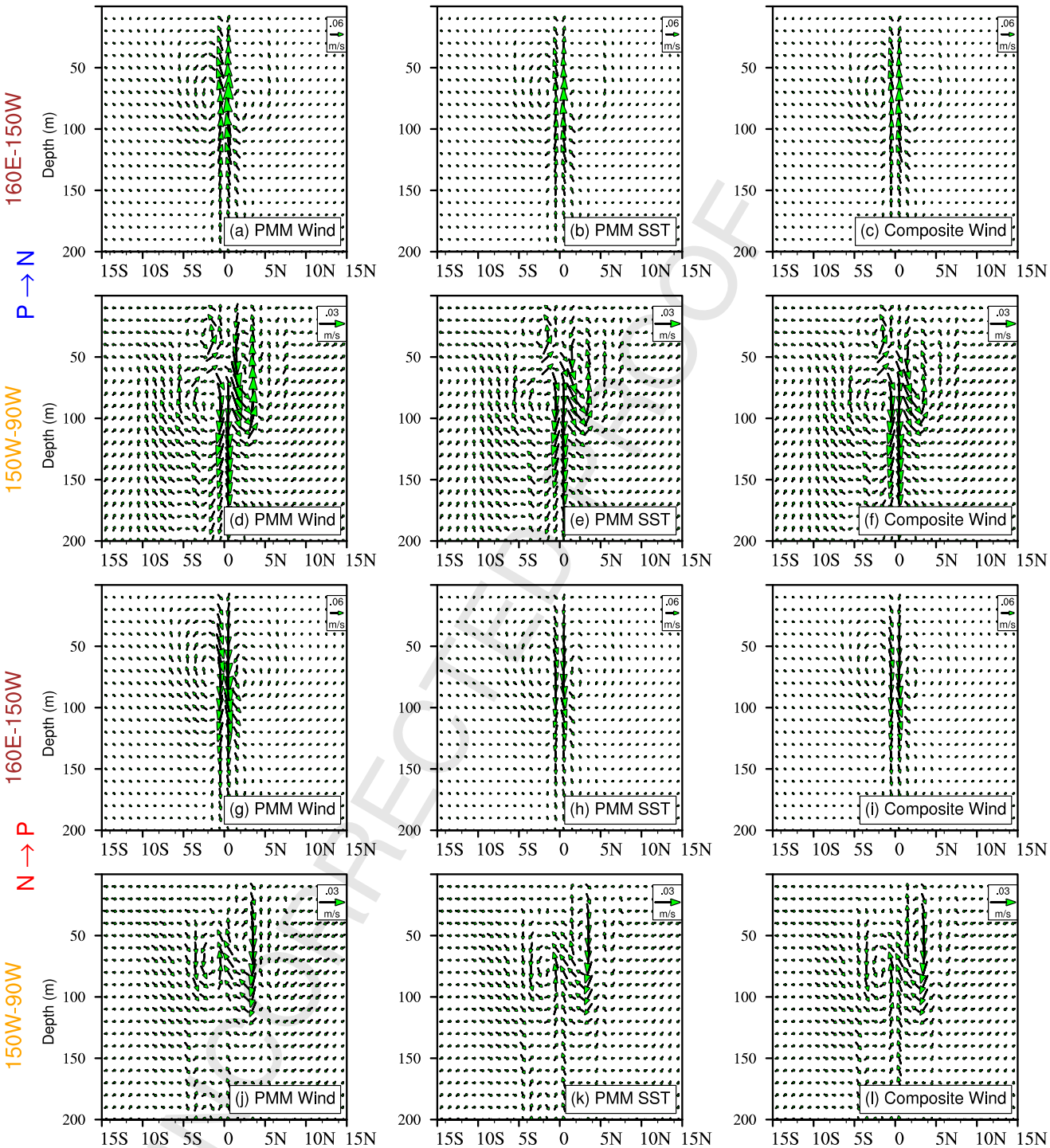

Figure 4. Response of meridional and vertical (5×10^4) currents averaged between (a–c and g–i) 160°E-150°W and (d–f and j–l) 150°W-90°W to the imposed wind forcing associated with the (a)–(f) negative and (g–l) positive phases of PMM. PMM-associated wind fields are determined by (a, d, g, and j) regressing the 8–20 years bandpass filtered PMM wind index onto the 8–20 years bandpass filtered 10 m wind anomalies (b, e, h, and k) regressing the 8–20 years bandpass filtered PMM SST index onto the 8–20 years bandpass filtered 10 m wind anomalies, and (c, f, i, and l) extracting the composite wind anomalies 30 month after the phase transition.

region (the light green box in Figures 1e and 1f; the region between the last two vertical dashed lines in Figures 1k and 1l).

The above analysis suggests the dominant role of anomalous wind forcing in driving tropical ocean circulation anomalies (Zhang et al., 2022), as confirmed by the large wind differences above the Niño3 and Niño4 regions (Figure S5 in Supporting Information S1). To further investigate the primary driver behind subsurface current anomalies, we run the ocean-sea ice component of the Community Earth System Model version 1.2.2 (CESM1) (Hurrell et al., 2013) with the wind forcing associated with the PMM (Figure S14 in Supporting Information S1; see Text S1 in Supporting Information S1 for experiment design). During the transition from positive to negative phases of TPDV, the PMM induces strong anomalous vertical motion in the Niño4 region which strengthens the local decadal signal, as evidenced by the observed features in Figure 1 and the simulated current anomalies (Figures 4a–4c). In contrast, subsurface current anomalies in the Niño3 region are notably weaker and exhibit a different phase compared to those in the Niño4 region, thereby diminishing the decadal signal in the Niño3 region (Figures 4d–4f), consistent with the observed weaker SST variance in the Niño3 region (Figure S1 in Supporting Information S1). These could potentially explain the previous asymmetric finding in Zheng et al. (2021). Reversed patterns are evident during the transition from negative to positive phases of TPDV (Figures 4g–4l), reaffirming the pivotal role of PMM in shaping decadal-scale climate variability in the tropical Pacific, particularly in the Niño4 region (Figure S1a in Supporting Information S1). While the Niño4 subsurface current characteristics are relatively symmetric during transitions between positive and negative phases (both positive to negative and negative to positive) in both observation (Figure S15 in Supporting Information S1) and simulation (cf., Figures 4a–4c and 4g–4i), it is important to note that during negative to positive transitions, the simulated vertical current anomalies in the Niño3 region are weaker than during positive to negative phases (cf., Figures 4d–4f and 4j–4l). This asymmetric response of subsurface currents in the Niño3 region to PMM wind forcing is also evident in observations (Figure S16 in Supporting Information S1) and could relate to the asymmetric intensity of the wind-evaporation-SST feedback (Zheng et al., 2021). The physical causes behind this asymmetry require further investigation.

5. Conclusions and Discussion

We have demonstrated that both subsurface temperature anomalies and PMM play distinct roles in shaping decadal-scale climate variability in the tropical Pacific. Subsurface temperature anomalies primarily initiate phase reversal while the PMM becomes significant only after the phase transition of TPDV. Specifically, during the transition from positive to negative phase, the anomalous wind fields associated with the PMM induce anomalous upwelling and downwelling which contribute to the strengthening and weakening of subsurface-produced SSTAs in the Niño4 and Niño3 regions, respectively. As a result, the observed decadal-scale SSTAs variance is most pronounced in the Niño4 region compared to other equatorial Pacific areas. A schematic of the comprehensive mechanism of the TPDV phase transition and decadal equatorial variance distribution is shown in Figure S17 in Supporting Information S1 (modified from Figure 6 in San et al. (2024)).

The dynamical processes associated with the PMM in driving TPDV are consistent with previous studies emphasizing the pivotal role of PMM-induced ocean dynamics in generating equatorial Pacific interannual variances (Hu et al., 2023; Shi et al., 2024; Zhang et al., 2022). However, extratropical forcing can also contribute to equatorial SST variance through thermodynamical mechanisms (Di Lorenzo et al., 2015; Zhao et al., 2023), though this process appears to be asymmetric at the interannual timescale (Fan et al., 2021; Zheng et al., 2021). This suggests that the effect of PMM on equatorial SST variability via thermodynamical processes may be unstable, whereas the dynamical processes seem stable at both interannual and decadal timescales. While some studies suggest that the relationship between PMM and equatorial SST variability is unstable at the interannual timescale (Zheng et al., 2023), a recent study indicates that this relationship is most prominent at the decadal timescale (Tao et al., 2024), further supporting our finding of the key role of PMM in enhancing decadal SST variability. Additionally, Figures S2 and S3 in Supporting Information S1 reveal a noticeable increase in the prominence of the decadal signal in the Niño3 region since the mid-2010s, suggesting a potential decadal regime shift toward the eastern Pacific. This feature will be explored in future studies.

Data Availability Statement

The PMM index. https://www.aos.wisc.edu/~dvimont/MModes/RealTime/PMM.RAW.txt.

The CESM1.2.2 code. https://www2.cesm.ucar.edu/models/cesm1.2/

Links to datasets used: HadISST1: https://www.metoffice.gov.uk/hadobs/hadisst/

NCEP-NCAR Reanalysis 1: https://psl.noaa.gov/data/gridded/data.ncep.reanalysis.html.

EN422: https://www.metoffice.gov.uk/hadobs/en4/download-en4-2-2.html.

GECCO3: https://www.cen.uni-hamburg.de/en/icdc/data/ocean/reanalysis-ocean/gecco3.html.

Acknowledgments
Computational resources were provided by the National Center for High-performance Computing (NCHC) of the National Applied Research Laboratories (NARLabs) in Taiwan. This research was supported by the NSTC Grant 112-2611-M-002-016-MY3, Taiwan.

References

Alexander, M. A., Bladé, I., Newman, M., Lanzante, J. R., Lau, N.-C., & Scott, J. D. (2002). The atmospheric bridge: The influence of ENSO teleconnections on air–sea interaction over the global oceans. *Journal of Climate*, *15*(16), 2205–2231. https://doi.org/10.1175/1520-0442(2002)015<2205:TABTIO>2.0.CO;2

Amaya, D. J. (2019). The pacific meridional mode and ENSO: A review. *Current Climate Change Reports*, *5*(4), 296–307. https://doi.org/10.1007/s40641-019-00142-x

Anderson, B. T., & Perez, R. C. (2015). ENSO and non-ENSO induced charging and discharging of the equatorial Pacific. *Climate Dynamics*, *45*(9), 2309–2327. https://doi.org/10.1007/s00382-015-2472-x

Anderson, B. T., Perez, R. C., & Karspeck, A. (2013). Triggering of El Niño onset through trade wind–induced charging of the equatorial Pacific. *Geophysical Research Letters*, *40*(6), 1212–1216. https://doi.org/10.1002/grl.50200

Andres, M., Park, J.-H., Wimbush, M., Zhu, X.-H., Nakamura, H., Kim, K., & Chang, K.-I. (2009). Manifestation of the pacific decadal oscillation in the Kuroshio. *Geophysical Research Letters*, *36*(16). https://doi.org/10.1029/2009GL039216

Ashok, K., Behera, S. K., Rao, S. A., Weng, H., & Yamagata, T. (2007). El Niño modoki and its possible teleconnection. *Journal of Geophysical Research*, *112*(C11). https://doi.org/10.1029/2006JC003798

Boucharel, J., Timmermann, A., Santoso, A., England, M. H., Jin, F.-F., & Balmaseda, M. A. (2015). A surface layer variance heat budget for ENSO. *Geophysical Research Letters*, *42*(9), 3529–3537. https://doi.org/10.1002/2015GL063843

Cai, W., Wu, L., Lengaigne, M., Li, T., McGregor, S., Kug, J.-S., et al. (2019). Pantropical climate interactions. *Science*, *363*(6430), eaav4236. https://doi.org/10.1126/science.aav4236

Capotondi, A., & Alexander, M. A. (2001). Rossby waves in the tropical North Pacific and their role in decadal thermocline variability. *Journal of Physical Oceanography*, *31*(12), 3496–3515. https://doi.org/10.1175/1520-0485(2002)031<3496:RWITTN>2.0.CO;2

Capotondi, A., Alexander, M. A., & Deser, C. (2003). Why are there Rossby wave maxima in the pacific at 10°S and 13°N? *Journal of Physical Oceanography*, *33*(8), 1549–1563. https://doi.org/10.1175/2407.1

Capotondi, A., McGregor, S., McPhaden, M. J., Cravatte, S., Holbrook, N. J., Imada, Y., et al. (2023). Mechanisms of tropical Pacific decadal variability. *Nature Reviews Earth and Environment*, *4*(11), 754–769. https://doi.org/10.1038/s43017-023-00486-x

Capotondi, A., Newman, M., Xu, T., & Di Lorenzo, E. (2022). An optimal precursor of northeast pacific marine heatwaves and central pacific El Niño events. *Geophysical Research Letters*, *49*(5), e2021GL097350. https://doi.org/10.1029/2021GL097350

Ceballos, L. I., Di Lorenzo, E., Hoyos, C. D., Schneider, N., & Taguchi, B. (2009). North pacific gyre oscillation synchronizes climate fluctuations in the eastern and western boundary systems. *Journal of Climate*, *22*(19), 5163–5174. https://doi.org/10.1175/2009JCLI2848.1

Chiang, J. C. H., & Vimont, D. J. (2004). Analogous pacific and atlantic meridional modes of tropical atmosphere–ocean variability. *Journal of Climate*, *17*(21), 4143–4158. https://doi.org/10.1175/JCLI4953.1

Chunhan, J., Bin, W., & Jian, L. (2021). Emerging pacific quasi-decadal oscillation over the past 70 years. *Geophysical Research Letters*, *48*(2), e2020GL090851. https://doi.org/10.1029/2020GL090851

Cibot, C., Maisonnave, E., Terray, L., & Dewitte, B. (2005). Mechanisms of tropical Pacific interannual-to-decadal variability in the ARPEGE/ORCA global coupled model. *Climate Dynamics*, *24*(7), 823–842. https://doi.org/10.1007/s00382-004-0513-y

Clarke, A. J., Van Gorder, S., & Colantuono, G. (2007). Wind stress curl and ENSO discharge/recharge in the equatorial pacific. *Journal of Physical Oceanography*, *37*(4), 1077–1091. https://doi.org/10.1175/JPO3035.1

Di Lorenzo, E., Liguori, G., Schneider, N., Furtado, J. C., Anderson, B. T., & Alexander, M. A. (2015). ENSO and meridional modes: A null hypothesis for pacific climate variability. *Geophysical Research Letters*, *42*(21), 9440–9448. https://doi.org/10.1002/2015GL066281

Di Lorenzo, E., Xu, T., Zhao, Y., Newman, M., Capotondi, A., Stevenson, S., et al. (2023). Modes and mechanisms of pacific decadal-scale variability. *Annual Review of Marine Science*, *15*(2023), 249–275. https://doi.org/10.1146/annurev-marine-040422-084555

Ding, R., Tseng, Y. H., Di Lorenzo, E., Shi, L., Li, J., Yu, J.-Y., et al. (2022). Multi-year El Niño events tied to the North Pacific oscillation. *Nature Communications*, *13*(1), 3871. https://doi.org/10.1038/s41467-022-31516-9

Duchon, C. E. (1979). Lanczos filtering in one and two dimensions. *Journal of Applied Meteorology and Climatology*, *18*(8), 1016–1022. https://doi.org/10.1175/1520-0450(1979)018<1016:LFIOAT>2.0.CO;2

Fan, H., Huang, B., Yang, S., & Dong, W. (2021). Influence of the pacific meridional mode on ENSO evolution and predictability: Asymmetric modulation and ocean preconditioning. *Journal of Climate*, *34*(5), 1881–1901. https://doi.org/10.1175/JCLI-D-20-0109.1

Fedorov, A. V., & Philander, S. G. (2000). Is El Niño changing? *Science*, *288*(5473), 1997–2002. https://doi.org/10.1126/science.288.5473.1997

Gan, B., Wang, T., Wu, L., Li, J., Qiu, B., Yang, H., & Zhang, L. (2023). A mesoscale ocean–atmosphere coupled pathway for decadal variability of the Kuroshio extension system. *Journal of Climate*, *36*(2), 485–510. https://doi.org/10.1175/JCLI-D-21-0557.1

Good, S. A., Martin, M. J., & Rayner, N. A. (2013). EN4: Quality controlled ocean temperature and salinity profiles and monthly objective analyses with uncertainty estimates. *Journal of Geophysical Research: Oceans*, *118*(12), 6704–6716. https://doi.org/10.1002/2013JC009067

Gu, D., & Philander, S. G. H. (1997). Interdecadal climate fluctuations that depend on exchanges between the tropics and extratropics. *Science*, *275*(5301), 805–807. https://doi.org/10.1126/science.275.5301.805

Hayashi, M., & Jin, F.-F. (2017). Subsurface nonlinear dynamical heating and ENSO asymmetry. *Geophysical Research Letters*, *44*(24), 12427–412435. https://doi.org/10.1002/2017GL075771

Hu, R., Lian, T., Feng, J., & Chen, D. (2023). Pacific meridional mode does not induce strong positive SST anomalies in the central equatorial pacific. *Journal of Climate*, *36*(12), 4113–4131. https://doi.org/10.1175/JCLI-D-22-0503.1

Huang, B., Xue, Y., Wang, H., Wang, W., & Kumar, A. (2012). Mixed layer heat budget of the El Niño in NCEP climate forecast system. *Climate Dynamics*, *39*(1), 365–381. https://doi.org/10.1007/s00382-011-1111-4

Hurrell, J. W., Holland, M. M., Gent, P. R., Ghan, S., Kay, J. E., Kushner, P. J., et al. (2013). The community Earth system model: A framework for collaborative research. *Bulletin of the American Meteorological Society*, *94*(9), 1339–1360. https://doi.org/10.1175/BAMS-D-12-00121.1

Joh, Y., & Di Lorenzo, E. (2019). Interactions between Kuroshio extension and central tropical pacific lead to preferred decadal-timescale oscillations in pacific climate. *Scientific Reports*, *9*(1), 13558. https://doi.org/10.1038/s41598-019-49927-y

Kalnay, E., Kanamitsu, M., Kistler, R., Collins, W., Deaven, D., Gandin, L., et al. (1996). The NCEP/NCAR 40-year reanalysis project. *Bulletin of the American Meteorological Society*, *77*(3), 437–472. https://doi.org/10.1175/1520-0477(1996)077<0437:TNYRP>2.0.CO;2

Kim, G.-I., & Kug, J.-S. (2020). Tropical pacific decadal variability induced by nonlinear rectification of El niño–southern oscillation. *Journal of Climate*, *33*(17), 7289–7302. https://doi.org/10.1175/JCLI-D-19-0123.1

Knutson, T. R., & Manabe, S. (1998). Model assessment of decadal variability and trends in the tropical Pacific ocean. *Journal of Climate*, *11*(9), 2273–2296. https://doi.org/10.1175/1520-0442(1998)011<2273:MAODVA>2.0.CO;2

Köhl, A. (2020). Evaluating the GECCO3 1948–2018 ocean synthesis – A configuration for initializing the MPI-ESM climate model. *Quarterly Journal of the Royal Meteorological Society*, *146*(730), 2250–2273. https://doi.org/10.1002/qj.3790

Lee, T., Fukumori, I., & Tang, B. (2004). Temperature advection: Internal versus external processes. *Journal of Physical Oceanography*, *34*(8), 1936–1944. https://doi.org/10.1175/1520-0485(2004)034<1936:TAIVEP>2.0.CO;2

Li, X., Xie, S.-P., Gille, S. T., & Yoo, C. (2016). Atlantic-induced pan-tropical climate change over the past three decades. *Nature Climate Change*, *6*(3), 275–279. https://doi.org/10.1038/nclimate2840

Liu, C., Zhang, W., Jin, F.-F., Stuecker, M. F., & Geng, L. (2022). Equatorial origin of the observed tropical pacific quasi-decadal variability from ENSO nonlinearity. *Geophysical Research Letters*, *49*(10), e2022GL097903. https://doi.org/10.1029/2022GL097903

Liu, C., Zhang, W., Stuecker, M. F., & Jin, F.-F. (2019). Pacific meridional mode-western North Pacific tropical cyclone linkage explained by tropical pacific quasi-decadal variability. *Geophysical Research Letters*, *46*(22), 13346–13354. https://doi.org/10.1029/2019GL085340

Liu, Z. (1994). A simple model of the mass exchange between the subtropical and tropical ocean. *Journal of Physical Oceanography*, *24*(6), 1153–1165. https://doi.org/10.1175/1520-0485(1994)024<1153:ASMOTM>2.0.CO;2

Liu, Z. (2012). Dynamics of interdecadal climate variability: A historical perspective. *Journal of Climate*, *25*(6), 1963–1995. https://doi.org/10.1175/2011JCLI3980.1

Liu, Z., & Alexander, M. (2007). Atmospheric bridge, oceanic tunnel, and global climatic teleconnections. *Reviews of Geophysics*, *45*(2). https://doi.org/10.1029/2005RG000172

Liu, Z., & Di Lorenzo, E. (2018). Mechanisms and predictability of pacific decadal variability. *Current Climate Change Reports*, *4*(2), 128–144. https://doi.org/10.1007/s40641-018-0090-5

Luo, J.-J., Sasaki, W., & Masumoto, Y. (2012). Indian Ocean warming modulates Pacific climate change. *Proceedings of the National Academy of Sciences*, *109*(46), 18701–18706. https://doi.org/10.1073/pnas.1210239109

McCreary, J. P., & Lu, P. (1994). Interaction between the subtropical and equatorial ocean circulations: The subtropical cell. *Journal of Physical Oceanography*, *24*(2), 466–497. https://doi.org/10.1175/1520-0485(1994)024<0466:IBTSAE>2.0.CO;2

McGregor, S., Timmermann, A., Stuecker, M. F., England, M. H., Merrifield, M., Jin, F.-F., & Chikamoto, Y. (2014). Recent Walker circulation strengthening and Pacific cooling amplified by Atlantic warming. *Nature Climate Change*, *4*(10), 888–892. https://doi.org/10.1038/nclimate2330

McPhaden, M. J., Lee, T., & McClurg, D. (2011). El Niño and its relationship to changing background conditions in the tropical Pacific Ocean. *Geophysical Research Letters*, *38*(15). https://doi.org/10.1029/2011GL048275

Meehl, G. A., & Hu, A. (2006). Megadroughts in the Indian monsoon region and southwest North America and a mechanism for associated multidecadal pacific Sea Surface temperature anomalies. *Journal of Climate*, *19*(9), 1605–1623. https://doi.org/10.1175/JCLI3675.1

Meehl, G. A., Teng, H., Capotondi, A., & Hu, A. (2021). The role of interannual ENSO events in decadal timescale transitions of the Interdecadal Pacific Oscillation. *Climate Dynamics*, *57*(7), 1933–1951. https://doi.org/10.1007/s00382-021-05784-y

Okumura, Y. M., DiNezio, P., & Deser, C. (2017). Evolving impacts of multiyear La niña events on atmospheric circulation and U.S. Drought. *Geophysical Research Letters*, *44*(22), 11614–611623. https://doi.org/10.1002/2017GL075034

Okumura, Y. M., Sun, T., & Wu, X. (2017). Asymmetric modulation of El Niño and La niña and the linkage to tropical pacific decadal variability. *Journal of Climate*, *30*(12), 4705–4733. https://doi.org/10.1175/JCLI-D-16-0680.1

Power, S., Lengaigne, M., Capotondi, A., Khodri, M., Vialard, J., Jebri, B., et al. (2021). Decadal climate variability in the tropical Pacific: Characteristics, causes, predictability, and prospects. *Science*, *374*(6563), eaay9165. https://doi.org/10.1126/science.aay9165

Qiu, B., Chen, S., Schneider, N., & Taguchi, B. (2014). A coupled decadal prediction of the dynamic state of the Kuroshio extension system. *Journal of Climate*, *27*(4), 1751–1764. https://doi.org/10.1175/JCLI-D-13-00318.1

Qiu, B., Schneider, N., & Chen, S. (2007). Coupled decadal variability in the North Pacific: An observationally constrained idealized model. *Journal of Climate*, *20*(14), 3602–3620. https://doi.org/10.1175/JCLI4190.1

Rayner, N. A., Parker, D. E., Horton, E. B., Folland, C. K., Alexander, L. V., Rowell, D. P., et al. (2003). Global analyses of sea surface temperature, sea ice, and night marine air temperature since the late nineteenth century. *Journal of Geophysical Research*, *108*(D14). https://doi.org/10.1029/2002JD002670

Rodgers, K. B., Friederichs, P., & Latif, M. (2004). Tropical pacific decadal variability and its relation to decadal modulations of ENSO. *Journal of Climate*, *17*(19), 3761–3774. https://doi.org/10.1175/1520-0442(2004)017<3761:TPDVAI>2.0.CO;2

San, S.-C., & Tseng, Y.-h. (2024). Aleutian low/PDO forces a decadal subsurface spiciness propagating mode in the North Pacific. *Climate Dynamics*, *62*(1), 703–721. https://doi.org/10.1007/s00382-023-06938-w

San, S.-C., Tseng, Y.-h., Ding, R., & Di Lorenzo, E. (2024). A key role of off-equatorial subsurface temperature anomalies in Tropical Pacific Decadal Variability. *npj Climate and Atmospheric Science*, *7*(1), 109. https://doi.org/10.1038/s41612-024-00643-z

Schneider, N. (2000). A decadal spiciness mode in the tropics. *Geophysical Research Letters*, *27*(2), 257–260. https://doi.org/10.1029/1999GL002348

Shi, L., Hu, S., & Ding, R. (2024). Relationship between NPO and multi-year El Niño events in a 2200 years simulation of CESM1. *Climate Dynamics*, *62*(5), 3539–3550. https://doi.org/10.1007/s00382-023-07079-w

Stuecker, M. F. (2018). Revisiting the pacific meridional mode. *Scientific Reports*, *8*(1), 3216. https://doi.org/10.1038/s41598-018-21537-0

Sullivan, A., Luo, J.-J., Hirst, A. C., Bi, D., Cai, W., & He, J. (2016). Robust contribution of decadal anomalies to the frequency of central-Pacific El Niño. *Scientific Reports*, *6*(1), 38540. https://doi.org/10.1038/srep38540

Sun, T., & Okumura, Y. M. (2020). Impact of ENSO-like tropical pacific decadal variability on the relative frequency of El Niño and La niña events. *Geophysical Research Letters*, *47*(3), e2019GL085832. https://doi.org/10.1029/2019GL085832

Taguchi, B., Xie, S.-P., Schneider, N., Nonaka, M., Sasaki, H., & Sasai, Y. (2007). Decadal variability of the Kuroshio extension: Observations and an eddy-resolving model hindcast. *Journal of Climate*, *20*(11), 2357–2377. https://doi.org/10.1175/JCLI4142.1

Tao, L., Xiao, Y., & Zhao, J. (2024). Relationship between the pacific meridional mode and El niño–southern oscillation on different timescales. *Atmospheric Research*, *302*, 107309. https://doi.org/10.1016/j.atmosres.2024.107309

Tatebe, H., Imada, Y., Mori, M., Kimoto, M., & Hasumi, H. (2013). Control of decadal and bidecadal climate variability in the tropical pacific by the off-equatorial south Pacific ocean. *Journal of Climate*, *26*(17), 6524–6534. https://doi.org/10.1175/JCLI-D-12-00137.1

Timmermann, A., An, S.-I., Kug, J.-S., Jin, F.-F., Cai, W., Capotondi, A., et al. (2018). El niño–southern oscillation complexity. *Nature*, *559*(7715), 535–545. https://doi.org/10.1038/s41586-018-0252-6

Trenberth, K. E., Branstator, G. W., Karoly, D., Kumar, A., Lau, N.-C., & Ropelewski, C. (1998). Progress during TOGA in understanding and modeling global teleconnections associated with tropical sea surface temperatures. *Journal of Geophysical Research*, *103*(C7), 14291–14324. https://doi.org/10.1029/97JC01444

Vialard, J., Menkes, C., Boulanger, J.-P., Delecluse, P., Guilyardi, E., McPhaden, M. J., & Madec, G. (2001). A model study of oceanic mechanisms affecting equatorial pacific Sea Surface temperature during the 1997–98 El Niño. *Journal of Physical Oceanography*, *31*(7), 1649–1675. https://doi.org/10.1175/1520-0485(2001)031<1649:AMSOOM>2.0.CO;2

Vimont, D. J. (2005). The contribution of the interannual ENSO cycle to the spatial pattern of decadal ENSO-like variability. *Journal of Climate*, *18*(12), 2080–2092. https://doi.org/10.1175/JCLI3365.1

Vimont, D. J., Battisti, D. S., & Hirst, A. C. (2001). Footprinting: A seasonal connection between the tropics and mid-latitudes. *Geophysical Research Letters*, *28*(20), 3923–3926. https://doi.org/10.1029/2001GL013435

Vimont, D. J., Battisti, D. S., & Hirst, A. C. (2003). The seasonal footprinting mechanism in the CSIRO general circulation models. *Journal of Climate*, *16*(16), 2653–2667. https://doi.org/10.1175/1520-0442(2003)016<2653:TSFMIT>2.0.CO;2

Wang, S.-Y., Gillies, R. R., Hipps, L. E., & Jin, J. (2011). A transition-phase teleconnection of the Pacific quasi-decadal oscillation. *Climate Dynamics*, *36*(3), 681–693. https://doi.org/10.1007/s00382-009-0722-5

Wang, S.-Y., Gillies, R. R., Jin, J., & Hipps, L. E. (2010). Coherence between the great salt lake level and the pacific quasi-decadal oscillation. *Journal of Climate*, *23*(8), 2161–2177. https://doi.org/10.1175/2009JCLI2979.1

Wang, S.-Y., Hakala, K., Gillies, R. R., & Capehart, W. J. (2014). The Pacific quasi-decadal oscillation (QDO): An important precursor toward anticipating major flood events in the Missouri River Basin? *Geophysical Research Letters*, *41*(3), 991–997. https://doi.org/10.1002/2013GL059042

Wills, S. M., & Thompson, D. W. J. (2018). On the observed relationships between wintertime variability in kuroshio–oyashio extension Sea Surface temperatures and the atmospheric circulation over the North Pacific. *Journal of Climate*, *31*(12), 4669–4681. https://doi.org/10.1175/JCLI-D-17-0343.1

Xie, S.-P., & Philander, S. G. H. (1994). A coupled ocean-atmosphere model of relevance to the ITCZ in the eastern Pacific. *Tellus A: Dynamic Meteorology and Oceanography*, *46*(4), 340–350. https://doi.org/10.3402/tellusa.v46i4.15484

Yu, J.-Y., & Fang, S.-W. (2018). The distinct contributions of the seasonal footprinting and charged-discharged mechanisms to ENSO complexity. *Geophysical Research Letters*, *45*(13), 6611–6618. https://doi.org/10.1029/2018GL077664

Zeller, M., McGregor, S., van Sebille, E., Capotondi, A., & Spence, P. (2021). Subtropical-tropical pathways of spiciness anomalies and their impact on equatorial Pacific temperature. *Climate Dynamics*, *56*(3), 1131–1144. https://doi.org/10.1007/s00382-020-05524-8

Zhang, R.-H., & Rothstein, L. M. (2000). Role of off-equatorial subsurface anomalies in initiating the 1991–1992 El Niño as revealed by the National Centers for Environmental Prediction ocean reanalysis data. *Journal of Geophysical Research*, *105*(C3), 6327–6339. https://doi.org/10.1029/1999JC900316

Zhang, R.-H., Rothstein, L. M., Busalacchi, A. J., & Liang, X.-Z. (1999). The onset of the 1991–92 El Niño event in the tropical Pacific Ocean: The NECC subsurface pathway. *Geophysical Research Letters*, *26*(7), 847–850. https://doi.org/10.1029/1999GL900111

Zhang, W., Jin, F.-F., Stuecker, M. F., Wittenberg, A. T., Timmermann, A., Ren, H.-L., et al. (2016). Unraveling El niño's impact on the east asian monsoon and yangtze river summer flooding. *Geophysical Research Letters*, *43*(21), 11375–311382. https://doi.org/10.1002/2016GL071190

Zhang, X., & McPhaden, M. J. (2010). Surface layer heat balance in the eastern equatorial Pacific ocean on interannual time scales: Influence of local versus remote wind forcing. *Journal of Climate*, *23*(16), 4375–4394. https://doi.org/10.1175/2010JCLI3469.1

Zhang, Y., Yu, S.-Y., Xie, S.-P., Amaya, D. J., Peng, Q., Kosaka, Y., et al. (2022). Role of ocean dynamics in equatorial Pacific decadal variability. *Climate Dynamics*, *59*(7), 2517–2529. https://doi.org/10.1007/s00382-022-06312-2

Zhao, M., Hendon, H. H., Alves, O., Liu, G., & Wang, G. (2016). Weakened eastern pacific El Niño predictability in the early twenty-first century. *Journal of Climate*, *29*(18), 6805–6822. https://doi.org/10.1175/JCLI-D-15-0876.1

Zhao, Y., & Di Lorenzo, E. (2020). The impacts of extra-tropical ENSO precursors on tropical pacific decadal-scale variability. *Scientific Reports*, *10*(1), 3031. https://doi.org/10.1038/s41598-020-59253-3

Zhao, Y., Di Lorenzo, E., Newman, M., Capotondi, A., & Stevenson, S. (2023). A pacific tropical decadal variability challenge for climate models. *Geophysical Research Letters*, *50*(15), e2023GL104037. https://doi.org/10.1029/2023GL104037

Zheng, Y., Chen, S., Chen, W., & Yu, B. (2023). A continuing increase of the impact of the spring North Pacific meridional mode on the following winter El Niño and southern oscillation. *Journal of Climate*, *36*(2), 585–602. https://doi.org/10.1175/JCLI-D-22-0190.1

Zheng, Y., Chen, W., Chen, S., Yao, S., & Cheng, C. (2021). Asymmetric impact of the boreal spring pacific meridional mode on the following winter El niño-southern oscillation. *International Journal of Climatology*, *41*(6), 3523–3538. https://doi.org/10.1002/joc.7033

Zhong, W., Zheng, X.-T., & Cai, W. (2017). A decadal tropical Pacific condition unfavorable to central Pacific El Niño. *Geophysical Research Letters*, *44*(15), 7919–7926. https://doi.org/10.1002/2017GL073846

Zuo, H., Balmaseda, M. A., Tietsche, S., Mogensen, K., & Mayer, M. (2019). The ECMWF operational ensemble reanalysis–analysis system for ocean and sea ice: A description of the system and assessment. *Ocean Science*, *15*(3), 779–808. https://doi.org/10.5194/os-15-779-2019